Proceedings of the Canadian Society for Mechanical Engineering International Congress 2022
CSME Congress 2022
June 5-8, 2022, Edmonton, AB, Canada

Numerical Investigation of Aerosol Transmission in A Classroom

Mojtaba Zabihi[1], Ri Li[1*], Joshua Brinkerhoff [1], Jonathan Little[2], Jake Winkler[2]
[1]School of Engineering, Faculty of Applied Science, University of British Columbia, Kelowna, Canada
[2]School of Health and Exercise Sciences, Faculty of Health and Social Development, University of British Columbia, Kelowna, Canada
* Sunny.Li@ubc.ca

Abstract— it has been more than two years since the COVID-19 pandemic has changed our world. Schools cannot be closed forever and now it is the time for everyone to go back to work. Classrooms are among the highest risk places because of their nature. Where many students are sitting for hours and one infected person can pass the disease to many others because of the long exposure time. In this research a classroom occupied with 20 students and a lecturer is considered. An unsteady Computational Fluid Dynamics (CFD) simulation of two-phase flows based on a Discrete Phase Model (DPM) is carried out to study the spreading of aerosol and droplets in the classroom. The simulation includes momentum and heat between the particles and the air flow. All the 21 simulated humans in the classroom generate heat and also inhale and exhale to mimic living persons. The lecturer generates aerosols and droplets for 15 minutes and when he stops the simulation continues before the next class begins. Transport and surface deposition of various sizes of small aerosols (from 1 μm) and large droplets (up to100 μm) are studied. The result showed that the natural convection flow has a significant effect on the aerosol particles but not much on the large droplets. It has to be included in the numerical simulation of aerosol transport where humans are present in the room. Based on the fallow time study, it is recommended to schedule the lectures with at least a 20 minutes interval to minimize the risk of spread of airborne diseases.

Keywords: Aerosol transport; COVID-19; Numerical simulation; Classroom; Particle deposition; Natural convection.

INTRODUCTION

The recent COVID-19 pandemic reminded us that the human being's health can be in a big threat by the airborne respiratory diseases particularly when it comes into the indoor environment. There are different classification of virus transmission including human-human transmission, airborne transmission, and other means of transmission such as endogenous infection, common vehicle, and vector spread [1]. Humans spend most of their time indoors [2] and their exposure to particles which even have outdoor origin occurs mainly indoors [3]. Particles generated by infected humans can be inhaled directly or transmitted from contaminated surfaces [4]. In general, respiratory droplets and aerosols are generated during exhalation, talking, coughing, sneezing, and other activities [5, 6]. In ventilated indoor environments, some of the generated particles escape the room through AC returns, some deposit either on object surfaces or human's bodies in the room and others may be directly inhaled.

To reduce disease transmission, measures should be taken to somehow maximize the fraction of particles that exit the system and minimize aerosol inhalation and their deposition on people especially on arms and faces [7, 8]. It was found that the spread of infectious diseases is related to the distribution of air flow indoors and its circulation pattern [9-13]. In the past decades the importance of the aerosols dynamics took attention of many researchers to investigate aerosol transport in indoors including a space with dividers and shelves [14], two people standing in distance in a room [15], isolation room [16, 25, 13], toilet [17], urban spaces [18], walking person [19, 20], aircraft cabin [21], operating room [22, 23], door opening [24, 25, 13], prayer room [26] and many more. But little work has been done to investigate particle transmission in class rooms [27]. Despite all efforts, no study has been found by the authors which included living people effects. This study has included living people effects such as inhalation, exhalation and natural convection due to human temperature on the aerosol transport in indoor environment. On top of that the classroom geometry and all furniture and humans are realistic to avoid simplification errors. A classroom usually is being used for back-to-back lecture sessions with less than 10 minutes intervals. In medical spaces, one solution to mitigate the risk associated with Aerosol Generating Procedures (AGPs) is the implementation of an administrative control called fallow time. Following an AGP, a wait-time is undertaken and the operatory is left fallow prior to surface sterilization and the next patient being admitted. The fallow time technique assumes that the dental operatory is equipped with sufficient air change turnover, so that 90-99% of the air is circulated out and exchanged during the fallow time [28, 29]. Similar approach may be considered to be applied to the classrooms. One of the goals of the present study is to recommend a fallow time for classrooms.

A realistic relatively large classroom with a total volume of 450 m^3 is considered. The objective of this study is to simulate the aerosol and droplet size particle transport in this classroom

using computational fluid dynamics (CFD) to determine the escaped percentage though the AC returns, how many are inhaled by humans while they breathe and the deposited percentage and also their locations on desks, seats and other classroom and furniture surfaces or either different parts of the people how are attending the lecture. It is of interest to estimate the fallow time for a certain air change per hour (ACH) and calculate the suspended particle percentage over the time during and after a lecture.

METHODS

A. *Computational model*

A classroom geometry model was established based on one of the Engineering, Management and Education (EME) building classrooms (EME-1121) at the University of British Columbia, Okanagan campus. The classroom measured 16.9 m length × 10.5 m width × 2.6 m height. It has 74 seats and 13 desks for students and the lecturer. Two levels are 12.7 and 25.4 cm elevated from the floor and are protected by railings from the sides. Two projectors are mounted to the ceiling. There are two distributed AC supplies (large perforated plated on the side walls) and two AC returns to circulate the air in the classroom. The airflow through the AC supplies has temperature 17.85 ^{o}C and relative humidity 40%, and provides 17 ACH (Air Change per Hour) for the classroom. The classroom is occupied with 20 students and a lecturer. Fig. 1 shows the classroom futures and students identifications. All the 21 simulated humans in the classroom perform thermal effect by having skin and clothing temperatures and also inhale and exhale to mimic living persons. The skin temperature for the exposed parts of the bodies (head and arms) and the clothing temperature are considered to be 34.5 ^{o}C and 28 ^{o}C respectively. After reaching the steady state, transient simulation starts using the steady data as initial conditions. The lecturer generates aerosols and droplets for 15 minutes and when he stops, the computation continues for 30 minutes to simulate the fallow time before the next class begins. 5 µm and smaller particles are considered as aerosols and 10 µm and larger ones are droplets. Various sizes of small aerosols (from 1 µm) and large droplets (up to100 µm) are studied. Particles are being released from the lecturer's mouth at a total rate of 272 particles per second. More detailed information of particles for each size can be found in TABLE I.

TABLE I. PARTICLES SIZE AND NUMBERS

Particle size (micro meter)	Number particle/s	Number particles in 15 minutes
1	160	144000
5	60	54000
10	20	18000
20	16	14400
50	12	10800
100	4	3600
Total	272	244800

Humans inhale and exhale air with almost the same duration time in a relaxed and normal breathing condition. So that all the modeled humans in the classroom breathe with a sinusoidal pattern with a maximum velocity of 1.632 m/s and period of 4.05 seconds. 20 random numbers between 0 and 4.05 make random phase lagged breathing functions for the students. The exhaled humid air has temperature 34.85 ^{o}C and %80 relative humidity.

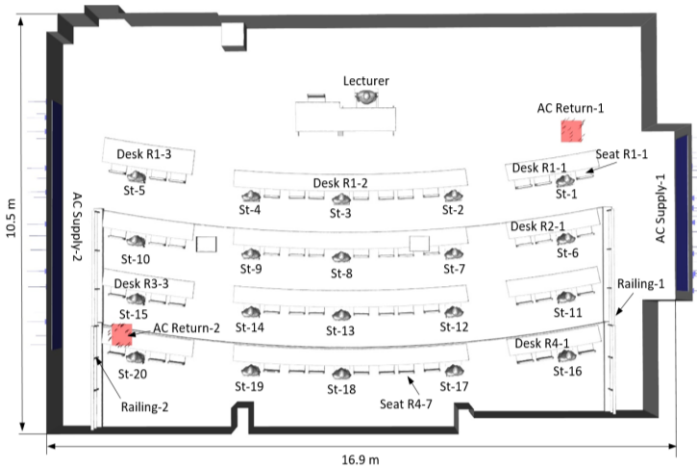

Figure 1. Classroom futures and students identifications

B. *Governing equations*

The flow to be modeled has two phases: a continuous phase and a discrete phase. The continuous phase is the gas flow, which is a binary mixture of air and vapor. Hereinafter, we will still call the continuous phase airflow, and the vapor content in air determines relative humidity. The discrete phase is the droplets emitted from the human's mouth. There are multiple flow sources in the room (AC supplies, particle flows and student's breathing flows) with different temperature and relative humidity. As a result, in addition to momentum transfer, the transports of energy and species also need to be solved.

Simulation is carried out using ANSYS-Fluent. The Euler-Lagrange approach is applied, and the Lagrangian discrete phase model is taken to track particles. This methodology is commonly used when interactions between droplets can be neglected.

Considering the many models provided by ANSYS-Fluent for turbulence calculations, k-ε and k-ω models are more practical for such a large computational domain as DNS and LES with a proper grid size and time steps are extremely costly. Among k-ε and k-ω models, the RNG k-ε [30, 31], Realizable k-ε [32, 33] and SST k-ω [34] turbulence have been recommended by other works because of their theoretically superiority to the other k-ε and k-ω models for these applications. For particle deposition simulations SST k-ω has shown better agreement with DNS and experimental data than RNG k-ε due to its smaller Lagrangian integral time scale in compression with the RNG k-ε model [35]. SST k-ω also predicted particle deposition closer to LES and experimental data than Realizable k-ε [36]. Therefore, it is more practical and accurate to use the SST k-ω turbulence models to calculate the continuous phase velocity field in our study. The series of governing equations for the continuous phase are the Unsteady Reynolds Averaged Naiver-Stokes equations (URANS) with

SST k-ω turbulence model closure which are well described in the literature [37].

Particles are tracked in the Lagragian frame of reference, and the motion is particle is governed by

$$m_p \frac{d\vec{u}_p}{dt} = m_p \frac{\vec{u}-\vec{u}_p}{\tau_r} + m_p \frac{\vec{g}(\rho_p - \rho)}{\rho_p} \quad (1)$$

Where m_p is the particle mass, $\vec{u}$ is the fluid phase velocity, $\vec{u}_p$ is the particle velocity, ρ is the fluid density, ρ_p is the density of the particle, $m_p \frac{\vec{u}-\vec{u}_p}{\tau_r}$ is the drag force, and τ_r is the particle relaxation time.

There is a simple heat balance equation to relate the particle temperature $T_p(t)$, to the convective heat transfer.

$$m_p c_p \frac{dT_p}{dt} = hA_p(T_\infty - T_p) \quad (2)$$

Where m_p is the mass of the particle, c_p is the heat capacity of the particle, A_p is the surface area of the particle, T_∞ is local temperature of the continuous phase and h is the convective heat transfer coefficient.

The turbulent dispersion of particles is predicted by integrating the trajectory equations for individual particles, using the instantaneous fluid velocity as expressed below:

$$u_i = \bar{u}_i + u_i' \quad (3)$$

The average velocity of the fluid $\bar{u}_i$ is obtained by the Unsteady Reynolds Averaged Naiver-Stokes equations (URANS) using the SST k-ω turbulence model. Based on a stochastic method called eddy lifetime or discrete random walk (DRW) model, the fluctuating component u_i' is assumed to be isotropic and to follow a Gaussian distribution, which can be obtained from (4).

$$u_i' = \zeta\sqrt{\frac{2}{3}k} \quad (4)$$

Where ζ is a normally distributed random number and k is the turbulent kinetic energy. Prediction of particle dispersion makes use of the concept of the integral time scale, T'. The integral time is proportional to the particle dispersion rate, as larger values indicate more turbulent motion in the flow the particle diffusivity is given by $\overline{u_i'u_j'}T'$.

For the small drift velocity the integral time scale of the particles becomes the fluid Lagrangian integral time scale, T_L. Using SST k-ω this time scale can be approximated as:

$$T_L = \frac{1.67}{\omega} \quad (5)$$

C. *Grid study*

Ansys-Meshing software is used for grid generation. A multi-grid mesh including a tetrahedron unstructured mesh for the bulk flow and a structured prism inflated layer for the boundary layer reign were adopted to discretize the geometry of the model. To capture the natural convection around the human bodies, the grid should be properly encrypted. So that different mesh sizes have applied to the complex human geometry and their surrounding computational domain.

To make sure the grid size effects on the simulation's results are negligible, five different numbers of grids are established to perform the grid study. Velocity magnitudes on two lines in the domain were extracted and compared. Line-1 is located vertically between the centroid of AC return-1 and the floor. Line-2 connects the Student-6's scalp to the ceiling. Line-1 and line-2 are shown in Fig. 2. Velocity magnitudes on two line-1 are shown in Fig. 3. The velocity magnitude contours, volumetric flow rate, maximum velocity magnitude, area-weighted average-vorticity magnitude and area-weighted average-helicity were investigated and compared for different number elements on a cut through plane at height H=1.75 m from the floor.

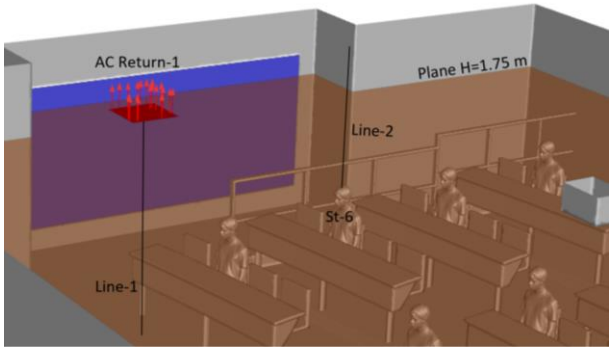

Figure 2. Grid study data extraxtion's locations

The relative difference between 40,354,589 elements and 30,237,771 elements cases for the volumetric flow rate, maximum velocity magnitude, area-weighted average-vorticity magnitude and area-weighted average-helicity were in an acceptable range in compression to the other cases. For saving computing resources and time cost 30,237,771 elements case is employed for the simulations.

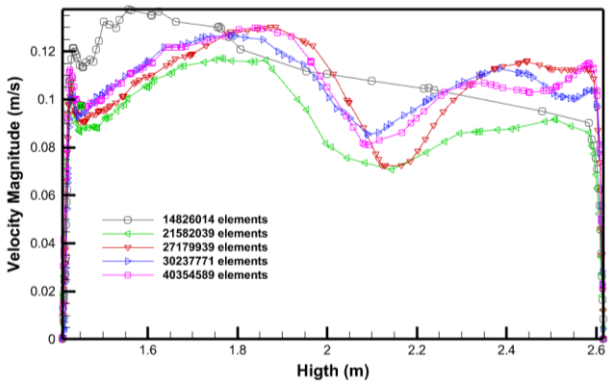

Figure 3. Velocity magnitudes on line-2 for different grids

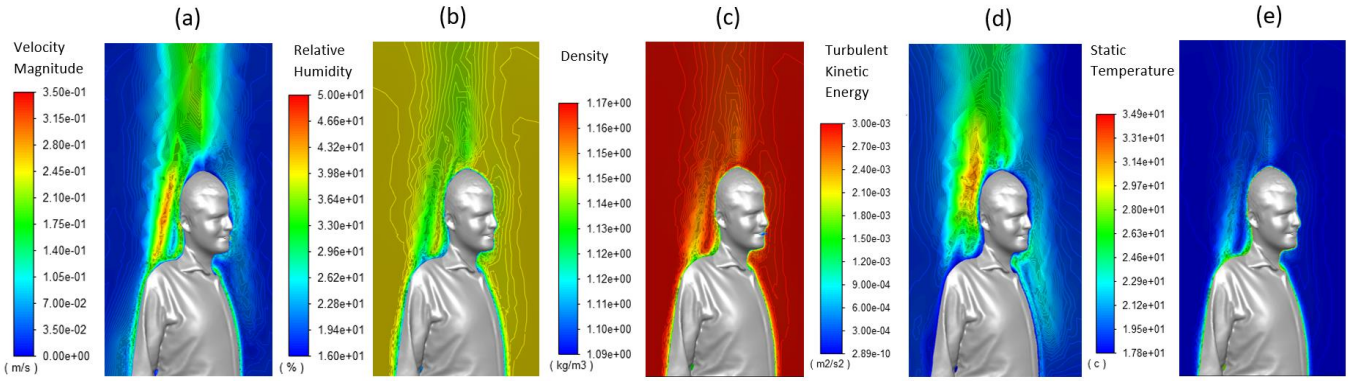

Figure 4. Contours of flow parameters around the lecturer. (a): Velocity magnitude, (b) Relative humidity, (c): Density, (d): Turbulent kinetic energy, (e): static temperature.

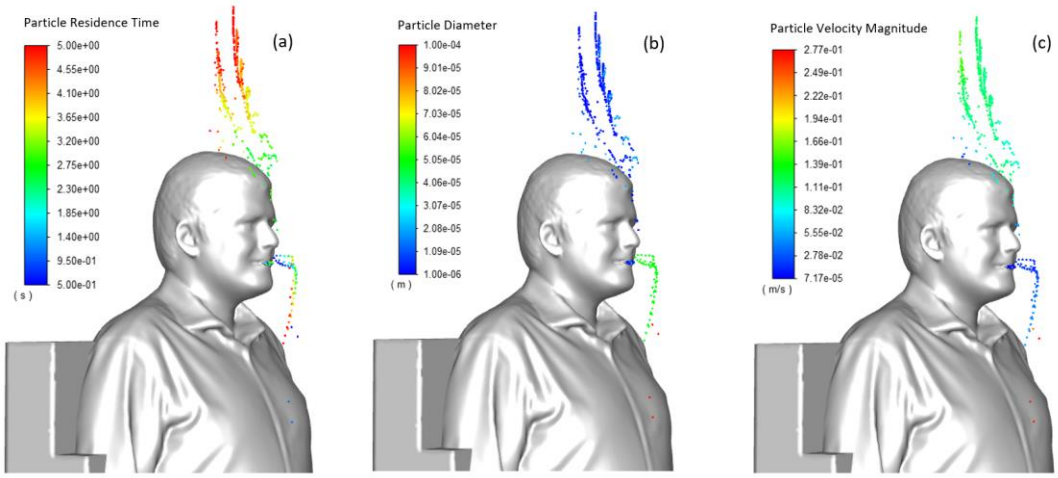

Figure 5. Particles at time = 5s. (a): Particle residence time, (b) particle diameter, (c): Particle velocity.

RESULTS AND DISCUSSION

Contours of the flow parameters such as velocity magnitude, relative humidity, density, turbulent kinetic energy and static temperature are shown in Fig. 4 the contours illustrate the distribution of the flow parameters on two perpendicular cutting planes showing the right profile and front view of the lecturer. Around the lecturer, the natural convection driven flow is much stronger than the background flow caused by AC circulation. The velocity magnitude above the human's shoulders can reach up to 10 times of its value for regions which are not affected by buoyancy forces. Density of the air decreases near the lecturer's body as the temperature increases. Turbulent kinetic energy is maximum where the annular plume generated by the warm body shears and slows down into the surrounding background air.

Fig. 5 illustrates the particles exhaled from lecturer's mouth after a breathing cycle. The particles are colored by (a): residence time, (b): diameter and (c): velocity magnitude at time = 5 seconds. The natural convection driven upward flow drags particles and the gravitational forces pull them down. The 1, 5, 10 µm particles easily have been suspended and dragged up, 20 µm particles go up but the gravitational forces make them slower than the others. 100 µm particles which are the heaviest ones fall down immediately. For 50 µm particles drag and gravitational forces are almost balanced at first and their initial momentum and horizontal convection drive the particles. When the particles enter the region which is less affected by natural convection they fall down and accelerate toward the ground.

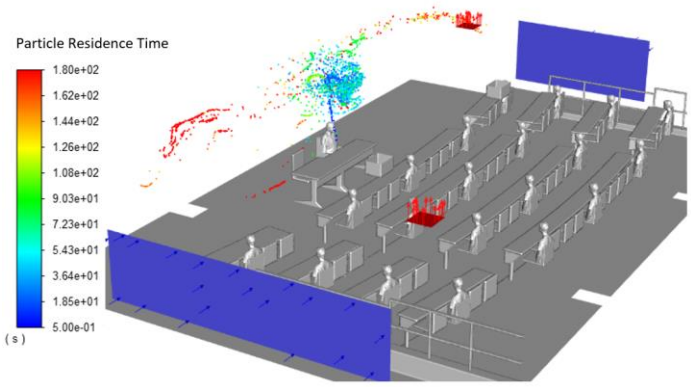

Figure 6. Particles at time = 3 minutes.

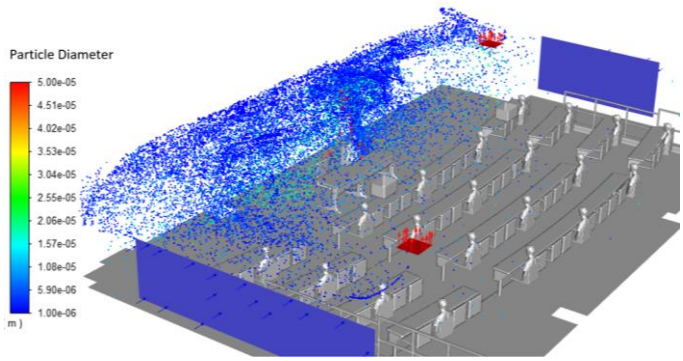

Figure 7. Particles at time = 10 minutes.

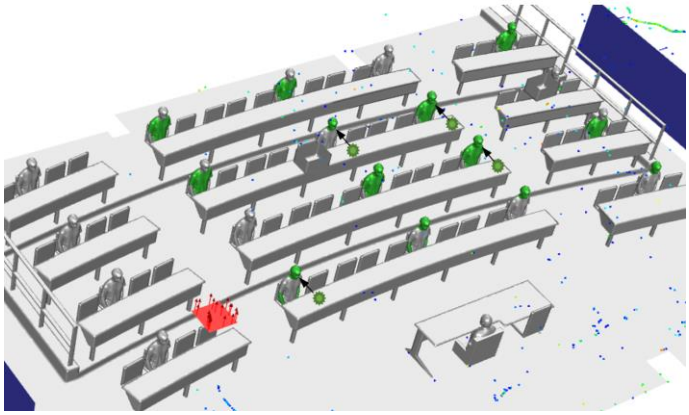

Figure 8. Particles at time = 30 minutes

Fig. 6 Shows the particles at t= 3 minutes, some of the aerosol particles (189 counts) already escaped from the classroom through the AC return-1. 7.7% of the total released particles have deposited on the lecturer lead. Suspended particle percentage for 1, 5, 10, 20, 50 and 100 µm particles are 97%, 95%, 94%, 49%, 41%, and 0.5% respectively. The particles distribution colored by the diameter at t= 10 minutes is shown in Figure 7. At this time almost none of the 50 µm particles have not reached farther than two meters from the mouth. So that by social distancing there is not a big concern about 50 and 100 µm particles in the classroom at this time. 20 µm ones can travel further but still have the tendency to settle down. The smaller particles are mostly still near the ceiling at this time and follow the bulk flow to travel around the classroom.

Fig. 8 Shows the situation at t= 30 minutes. The remaining particles are still nuclei in the air but are disappearing as more particles escape through the AC returns. The student's body parts which have been contacted with particles are indicated in green. The Four students who inhaled aerosols during the first 30 minutes are St-2, St-9, St-13 and St-14. Those student who are in the middle of the classroom are in the higher risk because of the aerosol circulation pattern. aerosols go up with the plume of natural convection flow, they circle around near the ceiling toward the AC returne-2 and then a good portion of them are being suck and mixt into the shear flow coming out of the AC suply-2 where the middle students are exposed to them so there is more chance for the aerosols to be inhaled or either be deposited on the body parts. None of the student who seat in front of the AC suply-1 have inhaled a particle or have a virus on their body and they are at the safest location of the classroom.

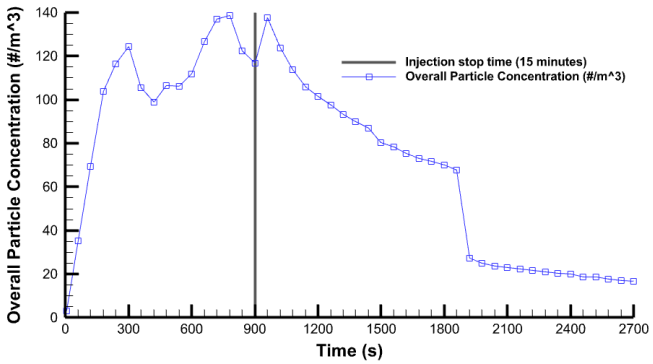

Figure 9. Overall particle concentration

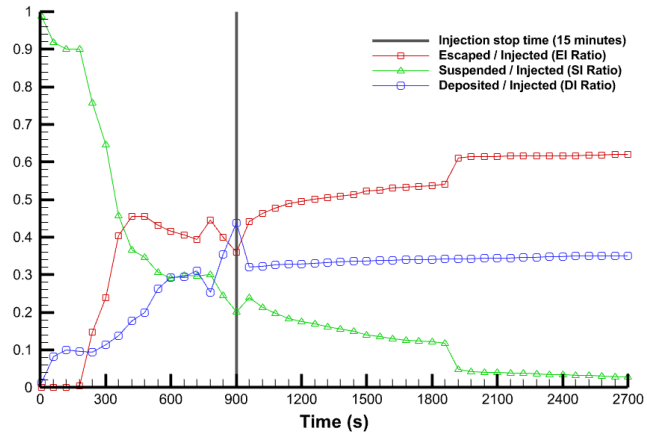

Figure 10. Particle ratios

Overall particle concentration and particle ratios over 45 minutes are shown in Fig. 9 and Fig. 10 respectively. The data for this classroom strongly recommends not to start the next lecture sooner than 20 minutes to let the AC change the air. Please note that the ACH for this classroom is relatively high and this fallow time could be much more for old standard buildings.

CONCLUSIONS

A transient numerical simulation has been carried out to investigate aerosol and droplet transport in a realistic classroom. From the simulation results it can be concluded that the natural convection plays the main role as the primary flow phenomena that determines the aerosol transport in a ventilated indoor environment. It has to be included in the numerical simulation of aerosol transport where humans are present in the room. In the region where natural convection is insignificant, aerosols are mainly affected by the ventilation airflow. The fallow time is not only important for the medical buildings but also it should come to the measures for the other public crowded spaces including schools. The fallow time for a high ACH ventilated classroom is recommended to be at least 20 minutes.

REFERENCES

[1] L. Morawska, "Drpolet fate in indoor environments, or can we prevent the spread of infection". Indoor Air, vol. 16(5), pp. 335-347, 2006.

[2] N.E. Klepeis, W. C. Nelson, W. R. Ott, J.P. Robinson, A. M. Tsang, P. Switzer, J. V. Behar, S. C. Hern, W.H. Engelmann, "The National Human Activity Pattern Survey (NHAPS): a resource for assessing exposure to environmental pollutants," Journal of Exposure Analysis and Environmental Epidemiology, vol. 11, pp. 231-252, 2001.

[3] C. Chen, B. Zhao, C. J. Weschler, "Indoor exposure to outdoor PM10: assessing its influence on the relationship between PM10 and short-term mortality in US cities," Epidemiology, vol. 23, pp. 870-878, 2012.

[4] M. Jayaweera, H. Perera, B. Gunawardana, J. Manatunge, "Transmission of COVID-19 virus by droplets and aerosols: A critical review on the unresolved dichotomy," Environmental Research, vol. 188, 109819, 2020.

[5] M. A. Kohanski, L. J. Lo, M. S. Waring, "Review of indoor aerosol generation, transport, and control in the context of COVID-19," International Forum of Allergy & Rhinology, vol. 10(10), pp. 1173–1179, 2020.

[6] P. Anfinrud, V. Stadnytskyi, C. E. Bax, A. Bax, "Visualizing speech-generated oral fluid droplets with laser light scattering," The New England Journal of Medicine, vol. 382(21), pp. 2061-2063, 2020.

[7] L. Morawska, J. W. Tang, W. Bahnfleth, P. M. Bluyssen, A. Boerstra, G. Buonanno, J. Cao, S. Dancer, A. Floto, F. Franchimon, C. Haworth, J. Hogeling, C. Isaxon, J. L. Jimenez, J. Kurnitski, Y. Li, M. Loomans, G. Marks, L. C. Marr, L. Mazzarella, A. K. Melikov, S. Miller, D. K. Milton, W. Nazaroff, P. V. Nielsen, C. Noakes, J. Peccia, X. Querol, C. Sekhar, O. Seppänen, S.-i. Tanabe, R. Tellier, K. W. Tham, P. Wargocki, A. Wierzbicka, and M. Yao, "How can airborne transmission of COVID-19 indoors be minimised?," Environment International, vol. 142, 105832, 2020.

[8] J. X. Wang, X. Cao, and Y. P. Chen, "An air distribution optimization of hospital wards for minimizing cross-infection," Journal of Cleaner Production, vol. 279, 123431, 2021.

[9] I. T. S. Yu, Y. Li, T. W. Wong, W. Tam, A. T. Chan, J. H. W. Lee, D. Y. C. Leung, T. Ho, "Evidence of airborne transmission of the severe acute respiratory syndrome virus," The New England journal of medicine, vol. 350(17), pp. 1731-1739, 2004.

[10] Y. Li, G. M. Leung, J. W. Tang, X. Yang, C. Y. H. Chao, J. Z. Lin, J. W. Lu, P. V. Nielsen, J. Niu, H. Qian, A. C. Sleigh, H. J. J. Su, J. Sundell, T. W. Wong, P. L. Yuen, "Role of ventilation in airborne transmission of infectious agents in the built environment-a multidisciplinary systematic review," Indoor Air, vol. 17, pp. 2-18, 2007.

[11] R. Gao, A. Li, "Dust deposition in ventilation and air-conditioning duct bend flows," Energy Conversion and Management, vol. 55, pp. 49-59, 2012.

[12] B. Zhao, Z. Zhang, X. Li, Numerical study of the transport of droplets or particles generated by respiratory system indoors," Building and Environment, vol. 40(8), pp. 1032-1039, 2005.

[13] Y. Tung, Y. Shih, S. Hu, "Numerical study on the dispersion of airborne contaminants from an isolation room in the case of door opening," Applied Thermal Engineering, vol. 29, pp. 1544-1551, 2009.

[14] V. Vuorinen, M. Aarnio, M. Alava, V. Alopaeus, N. Atanasova, M. Auvinen, N. Balasubramanian, H. Bordbar, P. Erästö, R. Grande, N. Hayward, A. Hellsten, S. Hostikka, J. Hokkanen, O. Kaario, A. Karvinen, I. Kivistö, M. Korhonen, R. Kosonen, J. Kuusela, S. Lestinen, E. Laurila, H. J. Nieminen, P. Peltonen, J. Pokki, A. Puisto, P. Råback, H. Salmenjoki, T. Sironen, M. Österberg, "Modelling aerosol transport and virus exposure with numerical simulations in relation to SARS-CoV-2 transmission by inhalation indoors," Safety Science,vol. 130, 104866, 2020.

[15] M. R. Pendar, J. C. Páscoa, "Numerical modeling of the distribution of virus carrying saliva droplets during sneeze and cough," Physics of Fluids, vol. 32, 083305, 2020.

[16] D. S. Thatiparti, U. Ghia, K. R. Mead, "Computational fluid dynamics study on the influence of an alternate ventilation configuration on the possible flow path of infectious cough aerosols in a mock airborne infection isolation room," Science and Technology for the Built Environment, vol. 23, pp. 355-366, 2017.

[17] Y. Y. Li, J. X. Wang, X. Chen, "Can a toilet promote virus transmission? From a fluid dynamics perspective," Physics of Fluids, vol. 32, 065107, 2020.

[18] A. M. Hassan , N. A. Megahed, "COVID-19 and urban spaces: A new integrated CFD approach for public health opportunities," Building and Environment, vol. 204, 108131, 2021.

[19] Y. Tao, K. Inthavong, J.Y. Tu, "Dynamic meshing modelling for particle resuspension caused by swinging manikin motion," Building and Environment, vol. 123, pp. 529-542, 2017.

[20] Z. Liu, M. Wu, H. Cao, Y. Wang, R. Rong, H. Zhu, "Influence of the visitor walking on airflow and the bioaerosol particles in typical open tomb chambers: an experimental and case study," Buildings, vol. 11. 538, 2021.

[21] W. Yan, Y. Zhang, Y. Sun, D. Li, "Experimental and CFD study of unsteady airborne pollutant transport within an aircraft cabin mock-up," Building and Environment, vol.44, pp. 34-43, 2009.

[22] C. Wang, S. Holmberg, S. Sadrizadeh, "Impact of door opening on the risk of surgical site infections in an operating room with mixing ventilation," Indoor and Built Environment., vol. 30(2), pp. 166-179, 2021.

[23] F. Romano, L. Marocco, J.Gusten, C. M. Joppolo, "Numerical and experimental analysis of airborne particles control in an operating theater," Building and Environment, vol. 89, pp. 369-379, 2015.

[24] J. Hendiger, M. Chludzińska, P. Ziętek, "Influence of the pressure difference and door swing on heavy contaminants migration between rooms," PLOS ONE, 0155159, 2016.

[25] P. E. Saarinen, P. Kalliomäki, J. W. Tang, H. Koskela, "Large eddy simulation of air Escape through a hospital isolation room single hinged doorway-validation by using tracer gases and simulated smoke videos," PLOS ONE, 0130667, 2015.

[26] D. A. Assaad, K. Ghali, N. Ghaddar, Particles dispersion due to human prostration cycle and ventilation system in a prayer room," Building and Environment, vol. 150, pp. 44-59, 2019.

[27] M. Abuhegazy, K. Talaat, O. Anderoglu, S.V. Poroseva, "Numerical investigation of aerosol transportin a classroom with relevance to COVID-19," Physics of Fluids, vol. 32, 103311, 2020.

[28] Ontario Agency for Health Protection and Promotion (Public Health Ontario), "COVID-19 in dental care settings," Queen's Printer for Ontario, Toronto, ON, 2020.

[29] CSA Group. CSA Z317.2:19, "Special requirements for heating, ventilation, and air-conditioning (HVAC) systems in health care facilities," CSA Group, Toronto, ON, 2019.

[30] T.L. Chan, G. Dong, C.W. Leung, "Validation of a two-dimensional pollutant dispersion model in an isolated street canyon," Atmos. Environ, vol. 36, pp. 861–872, 2002.

[31] Y. Tominaga, T. Stathopoulos, "Numerical simulation of dispersion around an isolated cubic building: comparison of various types of k-ε models," Atmospheric Environmen, vol. 43, pp. 3200-3210, 2009.

[32] Z. Liu, H. Liu, R. Rui, R. Rong, G. Cao, "Effect of a circulating nurse walking on airflow and bacteria-carrying particles in the operating room: An experimental and numerical study," Building and Environment, vol. 186, 107315, 2020.

[33] H. Yu, J. Th´e, "Simulation of gaseous pollutant dispersion around an isolated building using the kω-SST (shear stress transport) turbulence model," Journal of the Air & Waste Management Association, vol. 67(5), pp. 1096-2247, 2017.

[34] R. Ramponi, B. Blocken, "CFD simulation of cross-ventilation for a generic isolated building: Impact of computational parameters," Building and Environment, vol. 53, pp. 34-48, 2012.

[35] N. Gao, J. Niu, Q. He, T. Zhu, J. Wu, "Using RANS turbulence models and Lagrangian approach to predict particle deposition in turbulent channel flows," Building and Environment, vol. 48, pp. 206-214, 2012.

[36] Y. Tang, B. Guo, B. Ranjan, "Numerical simulation of aerosol deposition from turbulent flows using three-dimensional RANS and LES turbulence models," Engineering Applications of Computational Fluid Mechanics, vol. 9(1), pp. 174-186, 2015.

[37] Ansys-Fluent 2021R2 Theory Guide, Chapter 4: Turbulence, July 2021.